Accepted Manuscript

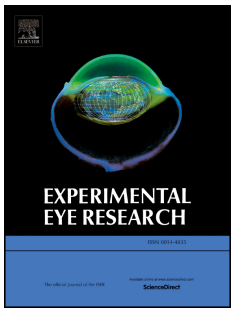

Diabetes induces changes in KIF1A, KIF5B and dynein distribution in the rat retina: Implications for axonal transport

Filipa I. Baptista, Maria J. Pinto, Filipe Elvas, Tiago Martins, Ramiro D. Almeida, António F. Ambrósio

PII: S0014-4835(14)00193-6

DOI: 10.1016/j.exer.2014.07.011

Reference: YEXER 6474

To appear in: *Experimental Eye Research*

Received Date: 1 March 2014

Revised Date: 14 July 2014

Accepted Date: 15 July 2014

Please cite this article as: Baptista, F.I., Pinto, M.J., Elvas, F., Martins, T., Almeida, R.D., Ambrósio, A.F., Diabetes induces changes in KIF1A, KIF5B and dynein distribution in the rat retina: Implications for axonal transport, *Experimental Eye Research* (2014), doi: 10.1016/j.exer.2014.07.011.

Research article

Diabetes induces changes in KIF1A, KIF5B and dynein distribution in the rat retina: Implications for axonal transport

Filipa I. Baptista[1,2], Maria J. Pinto[3,4], Filipe Elvas[1,2], Tiago Martins[1,2] Ramiro D. Almeida[3], António F. Ambrósio[1,2,3,5]

[1]Centre of Ophthalmology and Vision Sciences, IBILI, Faculty of Medicine, University of Coimbra, 3004-548 Coimbra, Portugal;

[2]Pharmacology and Experimental Therapeutics, IBILI, Faculty of Medicine, University of Coimbra, 3004-548 Coimbra, Portugal;

[3]CNC-Center for Neuroscience and Cell Biology, University of Coimbra, 3004-517 Coimbra, Portugal;

[4]PhD Programme in Experimental Biology and Biomedicine (PDBEB), Center for Neuroscience and Cell Biology, University of Coimbra, 3004-517 Coimbra, Portugal.

[5]AIBILI, 3004-548 Coimbra, Portugal.

Corresponding author:

António F. Ambrósio

Centre of Ophthalmology and Vision Sciences

IBILI, Faculty of Medicine

Azinhaga de Santa Comba

3004-548 Coimbra, Portugal

Phone: + 351 239 480 093

Fax: + 351 239 480 280

Email: afambrosio@fmed.uc.pt

Abbreviations

ANOVA, analysis of variance;

FBS, fetal bovine serum;

GCL, ganglion cell layer;

IL-1β, interleukin-1 beta;

INL, inner nuclear layer;

IPL, inner plexiform layer;

NMDA, *N*-Methyl-D-aspartate;

NO, nitric oxide;

OCT, optimal cutting temperature gel;

ONL, outer nuclear layer;

OPL, outer plexiform layer;

PBS, phosphate-buffered saline;

PFA, paraformaldehyde;

PHO, photoreceptor layer;

RGC, retinal ganglion cells;

RT, room temperature;

STZ, streptozotocin;

TBS, tris-buffered saline;

TBS-T, tris-buffered saline containing Tween-20;

TNF-α, tumor necrosis factor alpha;

TUJ-1, neuron-specific class III beta-tubulin.

Abstract

Diabetic retinopathy is a leading cause of vision loss and blindness. Disruption of axonal transport is associated with many neurodegenerative diseases and might also play a role in diabetes-associated disorders affecting nervous system. We investigated the impact of type 1 diabetes (2 and 8 weeks duration) on KIF1A, KIF5B and dynein

motor proteins in the retina. Additionally, since hyperglycemia is considered the main trigger of diabetic complications, we investigated whether prolonged exposure to elevated glucose could affect the content and distribution of motor proteins in retinal cultures. The immunoreactivity of motor proteins was evaluated by immunohistochemistry in retinal sections and by immunoblotting in total retinal extracts from streptozotocin-induced diabetic and age-matched control animals. Primary retinal cultures were exposed to high glucose (30 mM) or mannitol (osmotic control; 24.5 mM plus 5.5 mM glucose), for seven days. Diabetes decreased the content of KIF1A at 8 weeks of diabetes as well as KIF1A immunoreactivity in the majority of retinal layers, except for the photoreceptor and outer nuclear layer. Changes in KIF5B immunoreactivity were also detected by immunohistochemistry in the retina at 8 weeks of diabetes, being increased at the photoreceptor and outer nuclear layer, and decreased in the ganglion cell layer. Regarding dynein immunoreactivity there was an increase in the ganglion cell layer after 8 weeks of diabetes. No changes were detected in retinal cultures. These alterations suggest that axonal transport may be impaired under diabetes, which might contribute to early signs of neural dysfunction in the retina of diabetic patients and animal models.

Key words

Diabetes; retina; axonal transport; kinesin; dynein.

1. Introduction

Diabetic retinopathy is the most common microvascular complication of diabetes mellitus and is a leading cause of vision loss and blindness among working-age adults in Western countries. However, increasing evidence has shown that the neural components of the retina are also affected (Antonetti et al., 2006). Alterations in electroretinograms in diabetic patients and animals, and loss of colour and contrast sensitivity are early signs of neural dysfunction in the retina (Roy et al., 1986, Daley et

al., 1987, Sakai et al., 1995), demonstrating that the neural retina can be also affected by this disease.

Neurons are highly polarized cells, with long axons, which constitute a major challenge to the movement of proteins, vesicles, and organelles between cell bodies and presynaptic sites. To overcome this, neurons possess specialized transport machinery consisting of cytoskeletal motor proteins (kinesins and dynein) generating directed movements along cytoskeletal tracks. Axonal transport motor proteins require ATP demands, which implies the localization of functional mitochondria along the axons. Mobile mitochondria can become stationary or pause in regions that have a high metabolic demand and can move again rapidly in response to physiological changes. Defects in mitochondrial transport are implicated in the pathogenesis of several major neurological disorders (Sheng and Cai, 2012). Axonal transport is therefore crucial to maintain neuronal viability, and any impairment in this transport may play a role in the development or progression of several diseases (De Vos et al., 2008).

A decrease in the levels of mRNAs encoding for neurofilament proteins was found in the dorsal root ganglia of streptozocin-induced diabetic rats (Mohiuddin et al., 1995). Additionally, slow axonal transport of neurofilament and microtubule components is reduced, leading to a decrease in axonal caliber (Medori et al., 1988). These evidences suggest that deficits in axonal transport may contribute to neuronal changes observed in diabetes in neural tissues. To our knowledge, only a few studies have evaluated the effect of diabetes on axonal transport in the retina and most of them have focused in studying fluoro-gold labelling in retinal ganglion cells (RGCs) (Zhang et al., 1998, Ino-Ue et al., 2000, Zhang et al., 2000). Despite these evidences, the impact of diabetes in motor proteins (kinesins and dynein) in the retina has not been addressed. Nevertheless, potential changes in their content and distribution might underlie some changes already observed in axonal transport in the retina and visual pathway under diabetic conditions (Zhang et al., 2000, Fernandez et al., 2012).

Previously, we found that diabetes changes the levels of several synaptic proteins in retinal nerve terminals, with no changes in total retinal extracts, suggesting that axonal transport of those proteins may be impaired in diabetes (Gaspar et al., 2010a). Hyperglycemia is considered the main pathogenic factor for the development of diabetic complications. We found that high glucose leads to an accumulation of vesicular glutamate transporter-1, syntaxin-1 and synaptotagmin-1 at the cell body in hippocampal cell cultures, further suggesting that axonal transport of these proteins to nerve terminals might be affected under hyperglycemic conditions (Gaspar et al., 2010b). Recently, we showed that mRNA levels and the content of kinesin motor proteins are altered in the hippocampus of diabetic rats (Baptista et al., 2013). We also demonstrated that high glucose leads to changes in the immunoreactivity of motor proteins and synaptic proteins specifically in the axons of hippocampal neurons further suggesting that anterograde axonal transport may be impaired in the hippocampus (Baptista et al., 2013). These changes detected in the hippocampus of diabetic rats lead us to check whether similar changes could also be occurring in the retina under diabetes. Therefore, in this work, we aimed to study the effect of diabetes and also high glucose *per se* (prolonged exposure for 7 days), mimicking hyperglycemic conditions, on the content and distribution of the motor proteins KIF1A (kinesin that transports synaptic vesicle precursors), KIF5B (kinesin involved in mitochondrial transport and in the transport of synaptic vesicle precursors and membrane organelles) and dynein (motor protein for retrograde axonal transport) in diabetic animals and primary rat retinal cell cultures. Since motor proteins need ATP to carry cargoes along the axons, the distribution of mitochondria was also analyzed in retinal neural cell cultures exposed to high glucose.

2. Material and methods

2.1 Animals

Male Wistar rats (Charles River Laboratories), eight weeks-old, were randomly assigned to control or diabetic groups. All procedures were in agreement with the EU Directive 2010/63/EU for animal experiments. Diabetes was induced with a single intraperitoneal injection of streptozotocin (STZ; 65 mg/kg, freshly dissolved in 10 mM sodium citrate buffer, pH 4.5) (Sigma, St. Louis, MO, USA). Hyperglycemic status (blood glucose levels exceeding 250 mg/dl) was confirmed two days after STZ injection with a glucometer (Elite, Bayer, Portugal). Before sacrifice, rats were weighted and blood samples were collected for measurement of glucose. Diabetic rats and age-matched controls were anesthetized with halothane and then sacrificed, 2 and 8 weeks after the onset of diabetes.

2.2 Preparation of total retinal extracts

The eyes of diabetic and age-matched control animals were enucleated and placed in cold phosphate-buffered saline (PBS, in mM: 137 NaCl, 2.7 KCl, 10 Na_2HPO_4, 1.8 KH_2PO_4, pH 7.4, at 4ºC). Retinas were dissected and lysed in RIPA buffer (50 mM Tris–HCl, pH 7.4, 150 mM NaCl, 5 mM EDTA, 1% Triton X-100, 0.5% DOC, 0.1% SDS, 1 mM DTT) supplemented with complete miniprotease inhibitor cocktail tablets and phosphatase inhibitors (10 mM NaF and 1 mM Na_3VO_4). Then, lysates were sonicated and centrifuged at 16,000 x *g* for 10 min at 4ºC. The supernatant was collected and stored at -80ºC until use.

2.3 Primary cultures of rat retinal neural cells

Retinal cell cultures were obtained from the retinas of 3–5 days-old Wistar rats as previously described (Santiago et al., 2006). Cells were plated at a density of $2.0x10^6$ cells per cm^2 on poly-D-lysine substrate (0.1 mg/ml) and were maintained at 37ºC in a humidified incubator with 5% CO_2/air. The concentration of glucose in control conditions was 5 mM. After 2 days in culture, cells were incubated with 25 mM D-glucose (30 mM final concentration, with 5 mM from culture medium) or 25 mM D-

mannitol (plus 5 mM glucose from culture medium), which was used as an osmotic control, and maintained for additional 7 days in culture (nine days in culture).

2.4 Immunohistochemistry in retinal sections

2.4.1 Preparation of cryosections

Rats from each experimental group were deeply anesthetized with ketamine/xylazine and intracardially perfused with 0.1 M PBS, followed by 4% paraformaldehyde (PFA) in 0.1 M PBS. The eyes were enucleated, washed in ice-cold PBS and fixed in 4% PFA in PBS for 1 h. The cornea was removed and the posterior segments were fixed in 4% PFA in PBS for an additional period of 5 h. Tissue samples were transferred to 20% sucrose buffer overnight at 4℃ for cryoprotection and then were embedded in OCT (Shandon Cryomatrix, Shandon, USA). The blocks were stored in a deep freezer (-80ºC) until use. Transverse sections with 12 µm were obtained on a cryostat (Leica CM3050S, Nussloch, Germany) at -20ºC. The cryosections were then collected on gelatin-coated glass slides and allowed to air dry for 1 h. Retina sections were then stored at -20ºC for later use.

2.4.2 Immunohistochemistry

For immunostaining, frozen sections were placed 45 min at room temperature RT. After thawing, the sections were fixed in cold acetone (-20ºC) during 10 min and subsequently hydrated 3 times in PBS, during 10 min each time, to remove OCT. Sections were permeabilized with 0.25% Triton X-100 in PBS, for 30 min, and blocked with 5% fetal bovine serum (FBS) in PBS, for 30 min. Then, sections were incubated with primary antibodies (listed in Table 1) at 4℃, overnight, in a humid atmosphere, to avoid tissue dehydratation. After washing in PBS, a conjugated secondary antibody plus DAPI (1:5,000), to stain cell nuclei, were added for 1 h in the dark, at RT. After washing the sections in PBS, coverslips were mounted over the retinal sections using

glycergel (Dako mounting medium). Stained sections were observed with a laser scanning confocal microscope LSM 710 META (Zeiss, Germany).

2.4.3 Terminal deoxynucleotidyl transferase (TdT)-mediated dUTP nick-end labeling (TUNEL) assay

TUNEL assay was performed in retinal sections according to the manufacturer instructions (Promega, USA). Nuclei were counterstained with DAPI (1:5,000) and the sections were mounted using Dako glycergel mounting medium. TUNEL-positive cells were counted at the GCL, and expressed as an average from the four retinal sections per condition normalized to the retina length. Representative images were acquired with a laser scanning confocal microscope (Zeiss LSM 710).

2.4.4 Immunofluorescence quantification of retinal slices

A semi-quantitative determination of immunoreactive product densities at the level of the retinal layers was performed using ImageJ 1.42 software. In order to determine the fluorescence intensity of motor proteins (KIF1A, KIF5B and dynein), slides containing retinal slices from control and diabetic groups were blind coded. Sections from each immunohistological experiment, consisting of samples from control and diabetic group, were captured under identical conditions. Typically, four retinal sections from each animal were used for quantification. Random window sampling within the layers was carried out for quantification so that the intrinsic variability in the expression was appropriately quantified. To remove tissue background, for each image, a negative control (primary antibody omitted) of coverslipped tissue at the similar location was imaged, and background values were then subtracted from the experimental values, which were expressed in fluorescence arbitrary units (AU). Product densities were averaged across the four sections from each retina and expressed as mean percentage change; the percentage change across the control and diabetic groups was obtained and expressed as mean ± SEM. Although the intensity of staining varied from

one experiment to another, within a single experiment the application of primary and secondary antibodies, exposure times and acquisition image settings were uniform. This approach provides a measurement of the relative percentage change among control and diabetic groups based on the staining density in a given retinal layer.

2.5 RNA extraction and cDNA synthesis

Total RNA from the two retinas from control and diabetic rats was isolated using the RNeasy Mini Kit (Qiagen, Germany), as previously described (Baptista et al., 2013).

2.6 Primer design and Quantitative real time polymerase chain reaction

Primer design and evaluation for quantitative real time polymerase chain reaction (qRT-PCR) was performed exactly as previously described (Baptista et al., 2013). Final primer sequences and amplicon lengths are shown in Table 2.

qRT-PCR and data analysis were performed also as previously described (Baptista et al., 2013). The data analysis was based on 5 independent biological replicates per group. The results were expressed as the mean ± SEM. Data were analyzed by the unpaired Student's *t*-test (IBM SPSS Statistics, USA) to determine differences in gene expression between groups. Differences were considered statistically significant when $p<0.05$.

2.7 Preparation of extracts of cultured retinal cells

Cells were rinsed twice with ice-cold PBS and then lysed with RIPA buffer supplemented with complete miniprotease inhibitor cocktail tablets and phosphatase inhibitors. Lysates were incubated on ice for 30 min and then centrifuged at 16,100 x g for 10 min at 4ºC. The supernatant was collected and stored at -80ºC until use.

2.8 Western blot analysis

The protein concentration of each sample was determined by the bicinchoninic acid (BCA) protein assay (Pierce Biotechnology, Rockford, IL, USA). The samples were denaturated by adding 6x concentrated sample buffer (0.5 M Tris, 30% glycerol, 10% SDS, 0.6 M DTT, 0.012% bromophenol blue) and heating for 5 min at 95ºC. Equal amounts of protein were loaded into the gel and proteins were separated by sodium dodecyl sulphate-polyacrylamide gel electrophoresis (SDS-PAGE), using 6-8% gels. Proteins were transferred electrophoretically to PVDF membranes (Millipore, Billerica, Massachusetts, USA) and then the membranes were blocked with 5% low-fat milk in Tris-buffered saline (137 mM NaCl, 20 mM Tris-HCl, pH 7.6) containing 0.1% Tween-20 (TBS-T) for 1 h at room temperature. Membranes were incubated with primary antibodies (listed in Table 1) overnight at 4ºC. After washing for 1 h in TBS-T with 0.5% low-fat milk, the membranes were incubated with an anti-mouse or anti-goat alkaline phosphatase-linked IgG secondary antibody (1:10,000; GE Healthcare, Buckinghamshire, UK) in TBS-T with 1% low-fat milk for 1 h at room temperature. After washing for 1 h in TBS-T with 0.5% low-fat milk, the membranes were processed for protein detection using the enhanced chemifluorescence substrate (ECF; GE Healthcare). Fluorescence was detected on an imaging system (Thyphoon FLA 9000, GE Healthcare) and the digital quantification of bands immunoreactivity was performed using ImageQuant 5.0 software (Molecular Dynamics, Inc., Sunnyvale. CA, USA). The membranes were then reprobed and tested for β-actin immunoreactivity (1:5,000; Sigma) or β-III tubulin (1:5,000; Covance) to prove that similar amounts of protein were applied to the gels.

2.9 Immunocytochemistry

Retinal cell cultures were washed with PBS and fixed with 4% PFA and 4% sucrose for 10 min at RT. Cells were then washed and permeabilized with 1% Triton X-100 in PBS for 10 min at RT. Non-specific binding was prevented incubating cells with 5% FBS/0.2% Tween-20 in PBS for 20 min. Cells were incubated with the primary

antibodies (listed in Table 1) for 2 h at RT. After incubation, cells were rinsed with PBS and incubated with the secondary antibodies for 1 h at RT in the dark. The nuclei were stained with DAPI (1:5,000). Upon rinsing with PBS, the coverslips were mounted on glass slides using Dako Fluorescence mounting medium (Dako, Denmark). Preparations were visualized in a laser scanning confocal microscope LSM 710 META (Zeiss, Germany). Quantitative analysis of immunocytochemistry data was performed using ImageJ 1.42 software as previously described (Baptista et al., 2013).

2.10 Statistical analysis

Statistical comparisons between diabetic animals and respective age-matched controls were performed using the unpaired Student's *t*-test. Variance analysis was not undertaken since the effect of age on the content of motor proteins was not the aim of this study. Thus, gels were always loaded with samples from age-matched animals and not from animals with different ages. Statistical significance for the analysis of retinal cell cultures protein content was determined by using one-way ANOVA, followed by Dunnett's post hoc test. Quantitative analysis of immunofluorescence data was performed using ImageJ and statistical analysis between control and diabetic animals was performed using the unpaired Student's *t*-test. Differences were considered significant for $p<0.05$.

3. Results

3.1 Animal body weight and glucose blood levels

Animal body weight assessed prior the induction of diabetes was similar between the two groups (255.7±3.5 g for control animals and 253.4±3.4 g for diabetic group), as well as the blood glucose levels (89.1±1.4 mg/dl for controls and 86.7±5.7 mg/dl for diabetic group). The average weight and blood glucose levels for both diabetic and aged-matched control rats at the time of death are given in Table 3. A marked impairment in weight gain occurred in diabetic rats comparing to age-matched controls

in all time points analyzed. Diabetic animals also presented significantly higher blood glucose levels when compared to age-matched controls.

3.2 Diabetes decreases the protein levels of KIF1A in total retinal extracts

The impact of diabetes in motor proteins involved in axonal transport in the retina is unknown. We analyzed the mRNA levels and protein content of KIF1A, KIF5B, and dynein in total retinal extracts from diabetic animals and age-matched controls. At 2 weeks of diabetes, no significant changes were detected in the mRNA levels or protein content of KIF1A and KIF5B. However, a significant decrease was found at 8 weeks of diabetes in KIF1A protein levels in total retinal extracts (reduction to 69.6±6.0% of control), whereas KIF5B levels remained unchanged. Moreover, no significant differences were detected between diabetic and age-matched control animals in dynein mRNA levels or protein content at 2 and 8 weeks of diabetes (Figure 1).

3.3 Diabetes decreases KIF1A immunoreactivity

Immunoreactivity of KIF1A across the retinal layers was also analyzed in diabetic and age-matched control rats. No significant changes were observed in KIF1A immunoreactivity in the retina at 2 weeks of diabetes, compared to control. However, at 8 weeks of diabetes there was a significant decrease in KIF1A immunoreactivity in the majority of retinal layers (Figure 2). A reduction to 52.7±11.3%, 48.1±9.2%, 51.4±10.5% and 38.7±9.5% was detected in the outer plexiform layer (OPL), the inner nuclear layer (INL), the inner plexiform layer (IPL) and the ganglion cell layer (GCL), respectively.

3.4 Diabetes changes KIF5B immunoreactivity in the retina

No differences were found in the content of KIF5B in total retinal extracts or in the distribution of KIF5B at 2 weeks of diabetes. However, by immunohistochemistry it was detected a significant increase in KIF5B immunoreactivity in the outermost retinal

layers at 8 weeks of diabetes (Figure 3), namely at the outer and inner segments of photoreceptor layer (PHO) and at the outer nuclear layer (ONL), to 166.1±14.3% and 138.7±13.2%, respectively, comparing to age-matched controls. Conversely, a significant decrease in the GCL to 76.9±8.6%, comparing to age-matched controls, was detected at 8 weeks of diabetes (Figure 3).

3.5 Diabetes increases the dynein immunoreactivity at GCL

As mentioned before, in total retinal extracts, dynein levels remained similar to those found in control animals at 2 and 8 weeks of diabetes (Figure 1). Nevertheless, by immunohistochemistry, it was detected a significant increase (122.1±9.2% comparing to age-matched controls) in dynein immunoreactivity in the GCL at 8 weeks of diabetes (Figure 4).

3.6 High glucose does not change KIF1A, KIF5B, and dynein immunoreactivity in retinal cultures

Hyperglycemia is considered the main cause of diabetes complications, triggering various processes that may induce cell dysfunction. KIF1A and KIF5B are motor proteins that transport cargoes from the cell body to the synapse, whereas dynein is responsible for retrograde axonal transport. Exposure of cultured retinal cells to elevated concentrations of D-glucose (30 mM) or D-mannitol (24.5 mM + 5.5 mM glucose), for 7 days, did not induced changes in total protein content of KIFA, KIF5B and dynein (Figure 5A). Additionally, the morphology of retinal neurons was analyzed by immunocytochemistry using a TUJ-1 (neuron-specific class III β-tubulin) antibody. High glucose and mannitol did not induce any alteration in neuronal morphology (Figure 5B). The immunoreactivity of KIF1A, KIF5B and dynein, as well as the fluorescence of mitotracker (fluorescent dye that stains mitochondria in live cells) also showed that high glucose and mannitol did not induce any changes when compared to control (Figure 5B). Nevertheless, other factors besides hyperglycemia, such as the

increase in the levels of pro-inflammatory mediators, may possibly contribute for the changes detected in motor proteins in the retina of diabetic animals. In fact, inflammatory stimuli can induce changes in the levels of motor proteins in cultured retinal neural cells (Figure S1). KIF1A levels significantly decreased after exposure to IL-1β (10 ng/ml; reduction to 64.9±8% of control) or LPS (1 μg/ml; reduction to 76.6±7% of control) for 72h (Figure S1).

4. Discussion

In the current study, we evaluated the impact of diabetes and elevated glucose on key proteins involved in axonal transport in retinal cells. We show that diabetes alters the content of KIF1A and the distribution of KIF1A, KIF5B and dynein along retinal layers at 8 weeks of diabetes, suggesting that anterograde and retrograde transport mediated by these motor proteins may be impaired.

Previously, we have demonstrated that the mRNA levels and content of KIF1A and KIF5B motor proteins are altered in the hippocampus of diabetic rats. In this study, we found no correlation between protein and mRNA expression levels of KIF1A in the retina, indicating that the changes detected at protein level appear not to be caused by changes at the transcript level. Because there are various levels of post-transcriptional and post-translational regulation, the alterations in the transcript levels do not always correlate with the alterations observed at the protein levels, which is the case for KIF1A at least at these time points analyzed.

In a preceding study we have found a decrease in the content of several synaptic proteins important for neurotransmission in retinal nerve terminals at 2 and/or 8 weeks of diabetes (Gaspar et al., 2010a, Baptista et al., 2011). Since anterograde axonal transport is responsible for carrying proteins to nerve terminals, which are involved in synaptic transmission, the decrease in the content of synaptic proteins in nerve terminals may be a consequence of deficits in their transport. In fact, in cones lacking

KIF3A (kinesin present in photoreceptors), changes in photoreceptor properties occur, showing the importance of kinesin in the visual pathway (Avasthi et al., 2009). Moreover, trafficking of membrane proteins involved in phototransduction to the outer segments is impaired, resulting in progressive cone degeneration and absence of a photopic electroretinogram (Avasthi et al., 2009). Another study in the retina showed that, after 24 and 72 h of intravitreal injection of NMDA, an early elevation of KIF5B protein levels in the retina occurs, whereas a significant decrease is observed in the optic nerve, thus suggesting that a depletion of KIF5B precedes axonal degeneration of the optic nerve in NMDA-induced neurotoxicity (Kuribayashi et al., 2010). Moreover, it was found a deficit in the anterograde transport from the retina to the superior colliculus, 6 weeks after the induction of diabetes with STZ (Fernandez et al., 2012). Possibly, similar changes as those we detected in our diabetic model, namely in the content of KIF1A and distribution of KIF1A and KIF5B in the retinal layers at 8 weeks of diabetes, may also be occurring at 6 weeks of diabetes which may contribute therefore to the deficits observed in the anterograde transport from the retina to the superior colliculus.

In the opposite direction, there is the retrograde axonal transport system, which transports, among other molecules, neurotrophic factors that influence steady-state activities in the cell body. It was previously reported a progressive deficit in the retrograde axonal transport, mainly in large axons, that is evident 1 month after diabetes induction and is not associated with RGC loss (Ino-Ue et al., 2000). In an experimental model of glaucoma, the expression of dynein light chain in RGC is downregulated, which could contribute to neuronal dysfunction and apoptosis (van Oterendorp et al., 2011). On the other hand, it was demonstrated that dynein heavy chain (chain that contains the site of ATP hydrolysis and is the force-generating part of the protein) accumulates at the optic nerve head with experimental intraocular pressure elevation in the rat, supporting the hypothesis that disrupted axonal transport in RGC may be involved in the pathogenesis of glaucoma (Martin et al., 2006). Here, we

studied the 74 kDa dynein intermediate chain subunit that forms a bridge between the heavy chain and dynactin subunits, which bind microtubules and the cargo to be transported. We found that there is an increase in dynein immunoreactivity in the GCL of diabetic rats after 8 weeks duration. This increase in dynein immunoreactivity might be due to impairments at microtubule network level and/or impairment in dynein motor function, leading to an accumulation of dynein. An alternative explanation is that dynein is being trapped at the cell body due to lack of recycling back to the axon terminals by kinesin. It has been shown that kinesin and dynein motors can co-localize on vesicular cargoes (Hendricks et al., 2010, Encalada et al., 2011). Also, it was demonstrated that there are direct interactions between kinesin motors and components of the cytoplasmic dynein complex (Deacon et al., 2003, Ligon et al., 2004). Importantly, kinesin-dependent transport is required to deliver dynein to the plus ends of microtubules in the periphery (Zhang et al., 2003, Baumann et al., 2012). When axonal transport is blocked by ligature, kinesin accumulates in the proximal site, whereas dynein accumulates both proximally and distally, consistent with the fact that dynein is firstly transported down the axon in order to initiate active transport back to the cell body. The opposite does not occur, since kinesin motors do not accumulate on the distal side of a ligature, and so dynein does not transport kinesins as transport cargos (Li et al., 2000). These observations are a possible explanation for the decrease in KIF5B immunoreactivity in the GCL. Likely KIF5B levels decrease at the cell bodies of RGCs compromising anterograde transport. Consequently, dynein might be trapped at the cell body due to lack of recycling back to the axon terminals by kinesin, which might be the cause of the increase in the dynein immunoreactivity at the GCL after 8 weeks of diabetes. Regarding the KIF5B accumulation at the inner/outer segments and cell bodies of photoreceptors, it may be due to the imbalance in protein degradation and synthesis or to axonal transport deficit due to changes in tracks (e.g. microtubules) (De Vos et al., 2008). Alternatively, an overexpression of KIF5B may function as a compensatory mechanism as an attempt of the system to re-establish the protein

levels. It is important to highlight that the changes reported in motor proteins are not due to changes or loss in neuronal structure. We evaluated several neural elements of the retina to control for cell loss or cellular changes. Firstly, we performed a TUNEL assay in retinal slices from 8 weeks diabetic rats. In the majority of retinal slices, we did not find any TUNEL-positive cell. As it can be observed in Figure S2 A, in a few retinal slices of diabetic rats we detected just one TUNEL-positive cell. Regarding counts of DAPI-stained cells at the level of the GCL, we did not find any changes after 8 weeks of diabetes. Neural apoptosis in the GCL has already been reported on the whole-mounted diabetic rat retina (Barber et al., 1998). Barber and colleagues showed that an increase in the frequency of apoptosis occurred in whole-mounted rat retinas after 1, 3, 6, and 12 months of diabetes. They also reported a decrease in the RGC number and inner plexiform layer thickness, which occurs after 7.5 months of STZ-induced diabetes in rats (Barber et al., 1998), whereas Kusari et al. reported a loss of RGCs at 4 weeks of STZ injection (Kusari et al., 2007). Moreover, an increase in the number of apoptotic RGCs was also demonstrated after 3 months of diabetes (Seigel et al., 2006). In our hands, we only detected one TUNEL-positive cell in the RGC layer in just one slide and detected TUNEL-positive cells in the ONL in just a few slices, after 8 weeks of diabetes, indicating that in our model there is not a pronounced cell death in diabetic retinas at 8 weeks of diabetes. Besides TUNEL-positive cells and DAPI-stained cell counts, we also did not detect any changes in the number of Brn3a-positive cells (ganglion cell marker) after 8 weeks of diabetes (Figure S2 B). No significant changes were detected in beta-III-tubulin immunoreactivity at this timepoint as well (Figure S2 C).

Regarding potential macroglial changes, by analyzing GFAP immunoreactivity we did not find any significant changes in the levels of this protein neither by western blotting nor by immunohistochemistry (Figure S3 A). Barber et al. described that after 8 weeks of diabetes, there was a reduction in GFAP immunoreactivity in astrocytes and increased GFAP immunoreactivity in small groups of Muller cells (Barber et al., 2000).

In our retinal slices, immunoreactivity was largely confined to the ganglion cell layer and no differences in the immunoreactivity of GFAP were detected between control and diabetic animals. Concerning microglial cells, we found that there was an increased number of Iba-1-positive microglial cells in the retina of diabetic animals (21.7±1.9 for diabetic animals whereas age-matched controls presented 17.0±0.7 Iba-1-positive cells per mm of retina). Moreover, some cell bodies of Iba-1-positive cells appeared larger, with an amoeboid morphology, and with shorter processes in the retinas of diabetic animals (see inset in Figure S3 B), consistent with early microglia activation, as already had been described (Zeng et al., 2000, Barber et al., 2005, Gaucher et al., 2007) .

Previously, we demonstrate that the mRNA levels and content of KIF1A and KIF5B motor proteins are altered in the hippocampus of diabetic rats. Together, with the results presented in this study, we can suggest that diabetes may affect axonal transport at central nervous system, possibly by changing the transport of cargoes (namely synaptic vesicles and mitochondria) since their transport is mediated by these kinesins and dynein, and ultimately contribute to neural changes underlying diabetic encephalopathy and retinopathy.

Since hyperglycemia is considered the main factor underlying the development of diabetic complications, we evaluated whether prolonged exposure to high glucose *per se*, which simulates hyperglycemic conditions, could change the content of proteins involved in axonal transport in primary retinal cultures. Moreover, since KIF5 motors are responsible for the axonal transport of mitochondria, the fluorescence of mitotracker, a mitochondrial probe, was also evaluated. A decreased number of mitochondria in axons will likely decrease ATP supply to molecular motors, thus leading to decreased anterograde and retrograde movement of mitochondria and vesicles. High glucose did not induce any significant changes in the content and general distribution of motor proteins and mitochondria in retinal cultures. However, in this study we were not able to quantify the immunoreactivity of motor proteins

specifically in retinal neurons since we used mixed cultures and we were not able to isolate axons for quantification. Moreover, the neurons in these cultures are not viable in low density cultures, therefore we cannot completely discard the possibility that changes may be occurring specifically at the axonal level as we previously demonstrated in hippocampal neurons (Baptista et al., 2013).

On the other hand, we cannot exclude the hypothesis that other factors, besides hyperglycemia, such as the lack of insulin or the increase in the levels of pro-inflammatory mediators, may contribute for the changes in motor proteins detected in the retina of diabetic animals. In fact, in sensory neurons, the loss of insulin-dependent neurotrophic support may contribute to mitochondrial membrane depolarization, thus establishing a link between insulin and mitochondrial dysfunction in diabetic neuropathy (Fernyhough et al., 2003). Furthermore, retinal neurons depend on insulin receptor activity for survival (Barber et al., 2001). Long-term instability in retinal insulin signalling may impair insulin-dependent anabolic activities such as protein synthesis in the retina (Chihara, 1981) and increased cell death (Reiter and Gardner, 2003), suggesting that insulin signalling provides neurotrophic actions in the retina. Therefore, diabetic retinopathy may result in part from neurotrophin deficiency (Whitmire et al., 2011), similarly to peripheral neuropathy. In this study, retinal cells were cultured in the presence of fetal bovine serum, which makes impossible to address the question of the lack of insulin using these cell cultures. In fact, in the past, we tried to culture retinal cells without serum, using B27 supplement, but cultures did not differentiate properly and cells died.

Several evidences indicate that diabetic retinopathy also has characteristics of a low-grade chronic inflammatory disease and therefore, inflammation may also be a factor contributing to changes in axonal transport in diabetes. Increased production of cytokines, such as interleukin-1 beta (IL-1β) and tumor necrosis factor alpha (TNF-α), up-regulation of cyclooxygenase-2, increased expression of adhesion molecules and increased leukocyte adhesion and vascular permeability (Miyamoto et al., 1999, Carmo

et al., 2000, Kowluru et al., 2003) have been demonstrated in the retina of diabetic animals. Additionally, in the retinas of STZ-induced diabetic rats the levels of IL-1β are also increased (Carmo et al., 1999, Kowluru and Odenbach, 2004, Gerhardinger et al., 2005, Krady et al., 2005). Previously, it was shown that TNF-α induces perinuclear clustering of mitochondria in L929 cells. This clustering of mitochondria was microtubule-dependent and mimicked by immunoinhibition of conventional kinesin, therefore suggesting that TNF-α-induced mitochondrial clustering is caused by impaired kinesin-mediated transport of mitochondria (De Vos et al., 1998). Moreover, it was shown that TNF receptor-1 induces activation of kinase pathways, resulting in hyperphosphorylation of kinesin light chain and inhibition of kinesin activity (De Vos et al., 2000). In hippocampal neurons, nitric oxide released from activated microglia inhibits directed axonal movement of synaptic vesicle precursors containing synaptophysin and synaptotagmin (Stagi et al., 2005), and exposure of hippocampal neuronal cultures to TNF-α induces the dissociation of KIF5B from tubulin in axons and inhibits axonal transport of mitochondria and synaptophysin by reducing the mobile fraction via JNK (Stagi et al., 2006). Therefore, inflammatory cytokines may affect axonal transport motors and consequently contribute to the previous detected changes in synaptic proteins in the retina (Gaspar et al., 2010a, Baptista et al., 2011). Moreover, as an indication that inflammatory stimuli can induce changes in the levels of motor proteins, incubation of cultured retinal neural cells with IL-1β or LPS significantly decreased KIF1A levels, putting forward a possible explanation for the changes in KIF1A observed in the retinas of diabetic rats (Figure S1).

5. Conclusions

In summary, our data demonstrate that diabetes leads to changes in KIF1A, KIF5B and dynein motor proteins, which may contribute to impairments in anterograde and retrograde axonal transport and consequently to neuronal dysfunction in the retina. The

changes observed may be due to insulin deficiency or inflammation rather than hyperglycemia, or to a synergistic combination of these factors.

Acknowledgments

This work was supported by PEst-C/SAU/UI3282/2011-2013 and PEst-C/SAU/LA0001/2013-2014 (FCT, Portugal, and COMPETE). Filipa I. Baptista and Maria J. Pinto acknowledge fellowships from Fundação para a Ciência e a Tecnologia, Portugal (SFRH/BD/35961/2007 and SFRH/BD/51196/2010, respectively). Ramiro D. Almeida is supported by FEDER through COMPETE and by FCT (PTDC/SAU-NEU/104100/2008) and by Marie Curie Actions, 7th Framework Programme, EU.

Figure Legends

Figure 1. Diabetes decreases KIF1A protein content in the retina. The mRNA levels of KIF1A, KIF5B and dynein were assessed by RT-PCR (A), whereas protein levels were analyzed by immunoblotting (B) in total retinal extracts obtained from control and STZ-induced diabetic animals (2 and 8 weeks of diabetes). Representative Western blots are presented above the graphs, with the respective loading controls (β-actin or β-III tubulin), to confirm that identical amounts of protein from control and diabetic samples were loaded into the gel. The results are expressed as percentage of age-matched controls, and data are presented as mean ± SEM of 4-7 animals. *p<0.05, significantly different from control as determined by the unpaired Student's t-test.

Figure 2. Diabetes decreases KIF1A immunoreactivity along retinal layers. (A) The distribution of KIF1A was evaluated in retinas (retinal slices) isolated from control and STZ-induced diabetic animals (2 and 8 weeks of diabetes) by immunohistochemistry. Magnification 400x; Scale bar: 50 µm. *White arrows* indicate

the retinal layers where significant differences were detected comparing to age-matched controls. (B) The immunoreactivity of KIF1A was quantified in each retinal layer by ImageJ. The results are expressed as percentage of age-matched controls, and data are presented as mean ± SEM of at least 6 animals per condition. ***p<0.001, significantly different from control as determined by the unpaired Student's *t*-test**.**

Figure 3. Diabetes alters the distribution of KIF5B in the retina. (A) The distribution of KIF5B was evaluated in retinas (retinal slices) isolated from control and STZ-induced diabetic animals (2 and 8 weeks of diabetes) by immunohistochemistry. Magnification 400x; Scale bar: 50 µm. *White arrows*: significantly different from control. (B) The immunoreactivity of KIF5B was quantified in each retinal layer by ImageJ. The results are expressed as percentage of age-matched controls, and data are presented as mean ± SEM of at least 6 animals per condition. *p<0.05, **p<0.01, ***p<0.001, significantly different from control as determined by the unpaired Student's *t*-test**.**

Figure 4. Diabetes induces alterations in dynein immunoreactivity at GCL. (A) The distribution of dynein was evaluated in retinas (retinal slices) isolated from control and STZ-induced diabetic animals (2 and 8 weeks of diabetes) by immunohistochemistry. Magnification 400x; Scale bar: 50 µm. (B) The immunoreactivity of dynein was quantified in each retinal layer by ImageJ. The results are expressed as percentage of age-matched controls, and data are presented as mean ± SEM of at least 7 animals. ***p<0.05, significantly different from control as determined by the unpaired Student's *t*-test.

Figure 5. High glucose does not affect the content and distribution of KIF1A, KIF5B and dynein in retinal neural cell cultures. Cultured retinal cells were incubated with 25 mM D-glucose (final concentration 30 mM) or 25 mM D-mannitol (plus 5 mM glucose), which was used as an osmotic control, and maintained for

additional 7 days in culture. The concentration of glucose in control conditions was 5 mM. (A) The protein levels of KIF1A, KIF5B and dynein were analyzed by western blotting. Representative images of protein immunoreactive bands are presented above the graphs, with the respective loading control (β-actin or β-III tubulin). The densitometry of each band was analyzed and the results are expressed as percentage of control ± SEM, of five independent experiments. Regarding total protein content, statistical significance was determined by using ANOVA, followed by Dunnett's post hoc test. Differences were considered significant for $p<0.05$. (B) The protein levels and distribution of TUJ-1, KIF1A, KIF5B and dynein in the culture was analyzed by immunocytochemistry, as well as the intensity of fluorescence of mitotracker. Magnification 630x; Scale bar: 50 µm.

Supplementary Data

Figure Legend

Figure S1. Inflammatory stimuli induce changes in the content of KIF1A in retinal neural cell cultures. Cultured retinal cells were exposed to IL-1β (10 ng/ml) or lipopolysaccharide (LPS; 1µg/ml) for 24h or 72h. The protein levels of KIF1A, KIF5B and dynein were analyzed by western blotting. Representative images of protein immunoreactive bands are presented above the graphs, with the respective loading control (β-actin). The densitometry of each band was analyzed and the results are expressed as percentage of control ± SEM, of five independent experiments. Statistical significance was determined by using ANOVA, followed by Dunnett's post hoc test. *p<0.05, **p<0.01, significantly different from control.

Figure S2. Diabetes does not induce a widespread retinal degeneration after 8 weeks of diabetes. (A) Cell death was evaluated in retinal slices of 8 weeks diabetic rats by the TUNEL assay and by DAPI-stained cells counts at the GCL. TUNEL-positive cells can be identified by green fluorescence (white arrow), whereas DAPI-stained cells at

the GCL are in blue (yellow arrow). (B) Diabetes does not induce changes in the number of Brn3a-positive cells (red arrow) in the retina after 8 weeks of diabetes. (C) Diabetes does not induce changes in the immunoreactivity of beta-III tubulin in the retina after 8 weeks of diabetes. The protein levels of beta-III tubulin were analyzed by western blotting. Representative images of protein immunoreactive bands are presented above the graph. The results are expressed as percentage of age-matched controls, and data are presented as mean ± SEM of 8 animals. The distribution of beta-III tubulin was also evaluated in retinas (retinal slices) isolated from control and STZ-induced diabetic animals (8 weeks of diabetes) by immunohistochemistry and no significant differences were detected in beta-III tubulin immunoreactivity. Statistical significance was determined by using the unpaired Student's t-test.

Figure S3. Diabetes increases the number of Iba-1-positive cells in the retina after 8 weeks of diabetes, but not of GFAP-immunoreactivity. (A) The protein levels of GFAP were analyzed by western blotting. Representative images of protein immunoreactive bands are presented above the graph. The results are expressed as percentage of age-matched controls, and data are presented as mean ± SEM of 5 animals. Statistical significance was determined by using the unpaired Student's t-test. The quantification of GFAP immunoreactivity (in red) was evaluated in retinas (retinal slices) isolated from control and STZ-induced diabetic animals (8 weeks of diabetes) by immunohistochemistry. (B) Diabetes increases the number of Iba-1-positive cells in the retina after 8 weeks of diabetes. In some retinal slices some microglial cells present an amoeboid-like morphology contrasting with the ramified microglia morphology in control retinas. The distribution of Iba-1 positive cells (in red) was evaluated in retinas (retinal slices) isolated from control and STZ-induced diabetic animals (8 weeks of diabetes) by immunohistochemistry.

References

Antonetti DA, Barber AJ, Bronson SK, Freeman WM, Gardner TW, Jefferson LS, Kester M, Kimball SR, Krady JK, LaNoue KF, Norbury CC, Quinn PG, Sandirasegarane L, Simpson IA (2006) Diabetic retinopathy: seeing beyond glucose-induced microvascular disease. Diabetes 55:2401-2411.

Avasthi P, Watt CB, Williams DS, Le YZ, Li S, Chen CK, Marc RE, Frederick JM, Baehr W (2009) Trafficking of membrane proteins to cone but not rod outer segments is dependent on heterotrimeric kinesin-II. J Neurosci 29:14287-14298.

Baptista FI, Gaspar JM, Cristovao A, Santos PF, Kofalvi A, Ambrosio AF (2011) Diabetes induces early transient changes in the content of vesicular transporters and no major effects in neurotransmitter release in hippocampus and retina. Brain Res 1383:257-269.

Baptista FI, Pinto MJ, Elvas F, Almeida RD, Ambrosio AF (2013) Diabetes alters KIF1A and KIF5B motor proteins in the hippocampus. PloS one 8:e65515.

Barber AJ, Antonetti DA, Gardner TW (2000) Altered expression of retinal occludin and glial fibrillary acidic protein in experimental diabetes. The Penn State Retina Research Group. Invest Ophthalmol Vis Sci 41:3561-3568.

Barber AJ, Antonetti DA, Kern TS, Reiter CE, Soans RS, Krady JK, Levison SW, Gardner TW, Bronson SK (2005) The Ins2Akita mouse as a model of early retinal complications in diabetes. Invest Ophthalmol Vis Sci 46:2210-2218.

Barber AJ, Lieth E, Khin SA, Antonetti DA, Buchanan AG, Gardner TW (1998) Neural apoptosis in the retina during experimental and human diabetes. Early onset and effect of insulin. J Clin Invest 102:783-791.

Barber AJ, Nakamura M, Wolpert EB, Reiter CE, Seigel GM, Antonetti DA, Gardner TW (2001) Insulin rescues retinal neurons from apoptosis by a phosphatidylinositol 3-kinase/Akt-mediated mechanism that reduces the activation of caspase-3. J Biol Chem 276:32814-32821.

Baumann S, Pohlmann T, Jungbluth M, Brachmann A, Feldbrugge M (2012) Kinesin-3 and dynein mediate microtubule-dependent co-transport of mRNPs and endosomes. Journal of cell science 125:2740-2752.

Carmo A, Cunha-Vaz JG, Carvalho AP, Lopes MC (1999) L-arginine transport in retinas from streptozotocin diabetic rats: correlation with the level of IL-1 beta and NO synthase activity. Vision Res 39:3817-3823.

Carmo A, Cunha-Vaz JG, Carvalho AP, Lopes MC (2000) Effect of cyclosporin-A on the blood--retinal barrier permeability in streptozotocin-induced diabetes. Mediators of inflammation 9:243-248.

Chihara E (1981) Impairment of protein synthesis in the retinal tissue in diabetic rabbits: secondary reduction of fast axonal transport. Journal of neurochemistry 37:247-250.

Daley ML, Watzke RC, Riddle MC (1987) Early loss of blue-sensitive color vision in patients with type I diabetes. Diabetes Care 10:777-781.

De Vos K, Goossens V, Boone E, Vercammen D, Vancompernolle K, Vandenabeele P, Haegeman G, Fiers W, Grooten J (1998) The 55-kDa tumor necrosis factor receptor induces clustering of mitochondria through its membrane-proximal region. The Journal of biological chemistry 273:9673-9680.

De Vos K, Severin F, Van Herreweghe F, Vancompernolle K, Goossens V, Hyman A, Grooten J (2000) Tumor necrosis factor induces hyperphosphorylation of kinesin light chain and inhibits kinesin-mediated transport of mitochondria. J Cell Biol 149:1207-1214.

De Vos KJ, Grierson AJ, Ackerley S, Miller CC (2008) Role of axonal transport in neurodegenerative diseases. Annual review of neuroscience 31:151-173.

Deacon SW, Serpinskaya AS, Vaughan PS, Lopez Fanarraga M, Vernos I, Vaughan KT, Gelfand VI (2003) Dynactin is required for bidirectional organelle transport. The Journal of cell biology 160:297-301.

Encalada SE, Szpankowski L, Xia CH, Goldstein LS (2011) Stable kinesin and dynein assemblies drive the axonal transport of mammalian prion protein vesicles. Cell 144:551-565.

Fernandez DC, Pasquini LA, Dorfman D, Aldana Marcos HJ, Rosenstein RE (2012) Early distal axonopathy of the visual pathway in experimental diabetes. The American journal of pathology 180:303-313.

Fernyhough P, Huang TJ, Verkhratsky A (2003) Mechanism of mitochondrial dysfunction in diabetic sensory neuropathy. J Peripher Nerv Syst 8:227-235.

Gaspar JM, Baptista FI, Galvao J, Castilho AF, Cunha RA, Ambrosio AF (2010a) Diabetes differentially affects the content of exocytotic proteins in hippocampal and retinal nerve terminals. Neuroscience 169:1589-1600.

Gaspar JM, Castilho A, Baptista FI, Liberal J, Ambrosio AF (2010b) Long-term exposure to high glucose induces changes in the content and distribution of some exocytotic proteins in cultured hippocampal neurons. Neuroscience 171:981-992.

Gaucher D, Chiappore JA, Paques M, Simonutti M, Boitard C, Sahel JA, Massin P, Picaud S (2007) Microglial changes occur without neural cell death in diabetic retinopathy. Vision Res 47:612-623.

Gerhardinger C, Costa MB, Coulombe MC, Toth I, Hoehn T, Grosu P (2005) Expression of acute-phase response proteins in retinal Muller cells in diabetes. Invest Ophthalmol Vis Sci 46:349-357.

Hendricks AG, Perlson E, Ross JL, Schroeder HW, 3rd, Tokito M, Holzbaur EL (2010) Motor coordination via a tug-of-war mechanism drives bidirectional vesicle transport. Current biology : CB 20:697-702.

Ino-Ue M, Zhang L, Naka H, Kuriyama H, Yamamoto M (2000) Polyol metabolism of retrograde axonal transport in diabetic rat large optic nerve fiber. Invest Ophthalmol Vis Sci 41:4055-4058.

Kowluru RA, Koppolu P, Chakrabarti S, Chen S (2003) Diabetes-induced activation of nuclear transcriptional factor in the retina, and its inhibition by antioxidants. Free Radic Res 37:1169-1180.

Kowluru RA, Odenbach S (2004) Role of interleukin-1beta in the development of retinopathy in rats: effect of antioxidants. Invest Ophthalmol Vis Sci 45:4161-4166.

Krady JK, Basu A, Allen CM, Xu Y, LaNoue KF, Gardner TW, Levison SW (2005) Minocycline reduces proinflammatory cytokine expression, microglial activation, and caspase-3 activation in a rodent model of diabetic retinopathy. Diabetes 54:1559-1565.

Kuribayashi J, Kitaoka Y, Munemasa Y, Ueno S (2010) Kinesin-1 and degenerative changes in optic nerve axons in NMDA-induced neurotoxicity. Brain Res 1362:133-140.

Kusari J, Zhou S, Padillo E, Clarke KG, Gil DW (2007) Effect of memantine on neuroretinal function and retinal vascular changes of streptozotocin-induced diabetic rats. Invest Ophthalmol Vis Sci 48:5152-5159.

Li JY, Pfister KK, Brady ST, Dahlstrom A (2000) Cytoplasmic dynein conversion at a crush injury in rat peripheral axons. Journal of neuroscience research 61:151-161.

Ligon LA, Tokito M, Finklestein JM, Grossman FE, Holzbaur EL (2004) A direct interaction between cytoplasmic dynein and kinesin I may coordinate motor activity. The Journal of biological chemistry 279:19201-19208.

Martin KR, Quigley HA, Valenta D, Kielczewski J, Pease ME (2006) Optic nerve dynein motor protein distribution changes with intraocular pressure elevation in a rat model of glaucoma. Exp Eye Res 83:255-262.

Medori R, Jenich H, Autilio-Gambetti L, Gambetti P (1988) Experimental diabetic neuropathy: similar changes of slow axonal transport and axonal size in different animal models. J Neurosci 8:1814-1821.

Miyamoto K, Khosrof S, Bursell SE, Rohan R, Murata T, Clermont AC, Aiello LP, Ogura Y, Adamis AP (1999) Prevention of leukostasis and vascular leakage in streptozotocin-induced diabetic retinopathy via intercellular adhesion molecule-1 inhibition. Proc Natl Acad Sci U S A 96:10836-10841.

Mohiuddin L, Fernyhough P, Tomlinson DR (1995) Reduced levels of mRNA encoding endoskeletal and growth-associated proteins in sensory ganglia in experimental diabetes. Diabetes 44:25-30.

Reiter CE, Gardner TW (2003) Functions of insulin and insulin receptor signaling in retina: possible implications for diabetic retinopathy. Prog Retin Eye Res 22:545-562.

Roy MS, Gunkel RD, Podgor MJ (1986) Color vision defects in early diabetic retinopathy. Arch Ophthalmol 104:225-228.

Sakai H, Tani Y, Shirasawa E, Shirao Y, Kawasaki K (1995) Development of electroretinographic alterations in streptozotocin-induced diabetes in rats. Ophthalmic Res 27:57-63.

Santiago AR, Pereira TS, Garrido MJ, Cristovao AJ, Santos PF, Ambrosio AF (2006) High glucose and diabetes increase the release of [3H]-D-aspartate in retinal cell cultures and in rat retinas. Neurochem Int 48:453-458.

Seigel GM, Lupien SB, Campbell LM, Ishii DN (2006) Systemic IGF-I treatment inhibits cell death in diabetic rat retina. Journal of diabetes and its complications 20:196-204.

Sheng ZH, Cai Q (2012) Mitochondrial transport in neurons: impact on synaptic homeostasis and neurodegeneration. Nat Rev Neurosci 13:77-93.

Stagi M, Dittrich PS, Frank N, Iliev AI, Schwille P, Neumann H (2005) Breakdown of axonal synaptic vesicle precursor transport by microglial nitric oxide. J Neurosci 25:352-362.

Stagi M, Gorlovoy P, Larionov S, Takahashi K, Neumann H (2006) Unloading kinesin transported cargoes from the tubulin track via the inflammatory c-Jun N-terminal kinase pathway. FASEB J 20:2573-2575.

van Oterendorp C, Lorber B, Jovanovic Z, Yeo G, Lagreze WA, Martin KR (2011) The expression of dynein light chain DYNLL1 (LC8-1) is persistently downregulated in glaucomatous rat retinal ganglion cells. Exp Eye Res 92:138-146.

Whitmire W, Al-Gayyar MM, Abdelsaid M, Yousufzai BK, El-Remessy AB (2011) Alteration of growth factors and neuronal death in diabetic retinopathy: what we have learned so far. Mol Vis 17:300-308.

Zeng XX, Ng YK, Ling EA (2000) Neuronal and microglial response in the retina of streptozotocin-induced diabetic rats.PG - 463-71. Vis Neurosci 17.

Zhang J, Li S, Fischer R, Xiang X (2003) Accumulation of cytoplasmic dynein and dynactin at microtubule plus ends in Aspergillus nidulans is kinesin dependent. Molecular biology of the cell 14:1479-1488.

Zhang L, Ino-ue M, Dong K, Yamamoto M (2000) Retrograde axonal transport impairment of large- and medium-sized retinal ganglion cells in diabetic rat. Current eye research 20:131-136.

Zhang L, Inoue M, Dong K, Yamamoto M (1998) Alterations in retrograde axonal transport in optic nerve of type I and type II diabetic rats. The Kobe journal of medical sciences 44:205-215.

Table 1. List of primary antibodies used.

Primary Antibody	Sample	Antibody Dilution	Protein (µg)	Source
Mouse anti-KIF1A	Total Extracts Retina	1:1,000	40	BD Biosciences
	Total Extracts Primary cultures	1:1,000	40	
Goat anti-KIF1A	Immunocytochemistry	1:50	–	Santa Cruz
	Immunohistochemistry	1:50	–	
Goat anti-KIF5B	Total Extracts Retina	1:2,000	10	Abcam
	Immunohistochemistry	1:100	–	
	Total Extracts Primary cultures	1:2,000	20	
	Immunocytochemistry	1:100	–	
Mouse anti-Dynein	Total Extracts Retina	1:2,000	20	Abcam
	Immunohistochemistry	1:100	–	
	Total Extracts Primary cultures	1:2,000	40	
	Immunocytochemistry	1:100	–	
Rabbit anti-TUJ-1	Total Extracts Retina	1:5,000	10	Covance
	Immunocytochemistry	1:1,000	–	
Mouse anti-GFAP	Total Extracts Retina	1:5,000	10	Calbiochem
	Immunocytochemistry	1:400	–	
Rabbit anti-Iba-1	Immunocytochemistry	1:1,000	–	Wako
Mouse anti-Brn3a	Immunocytochemistry	1:200	–	Chemicon

Table 2. Primer sequences.

Gene	Forward primer (5'-3')	Reverse primer (5'-3')	Amplicon size (bp)
Reference genes			
GAPDH	GACTTCAACAGCAACTCC	GCCATATTCATTGTCATACCA	105
HPRT	ATGGGAGGCCATCACATTGT	ATGTAATCCAGCAGGTCAGCAA	77
YWHAZ	CAAGCATACCAAGAAGCATTTGA	GGGCCAGACCCAGTCTGA	76
Target genes			
KIF1A	CATTAGTTAGTGGCGTTGA	TACCTGGAGGCATTAGAAA	91
KIF5B	GTGATGATTGCGTCCAAG	CTTCTTTGCACAATCGTTG	90
DYNEIN	TTCTGGCGTAGTCCTATT	ACACCACATCTCAAGTCT	104

GAPDH - glyceraldehyde-3- phosphate dehydrogenase;

HPRT - human hypoxanthine phosphoribosyltransferase;

YWHAZ - tyrosine 3-monooxygenase/tryptophan 5-monooxygenase activation protein, zeta polypeptide;

KIF1A - kinesin family member 1A;

KIF5B - kinesin family member 5B;

DYNEIN - dynein cytoplasmic 1 intermediate chain.

Table 3. Average weight and blood glucose levels of diabetic and aged-matched control rats.

		Weight (g)	Blood Glucose (mg/dL)
2 Weeks	Control	319.5±5.4	102.3±3.5
	Diabetic	233.2±8.5***	377.4±21.2***
8 Weeks	Control	394.6±16.7	89.9±2.9
	Diabetic	245.7±13.6***	488.9±38.5***

Measurements were made immediately before the sacrifice of the animals. ***p<0.001.

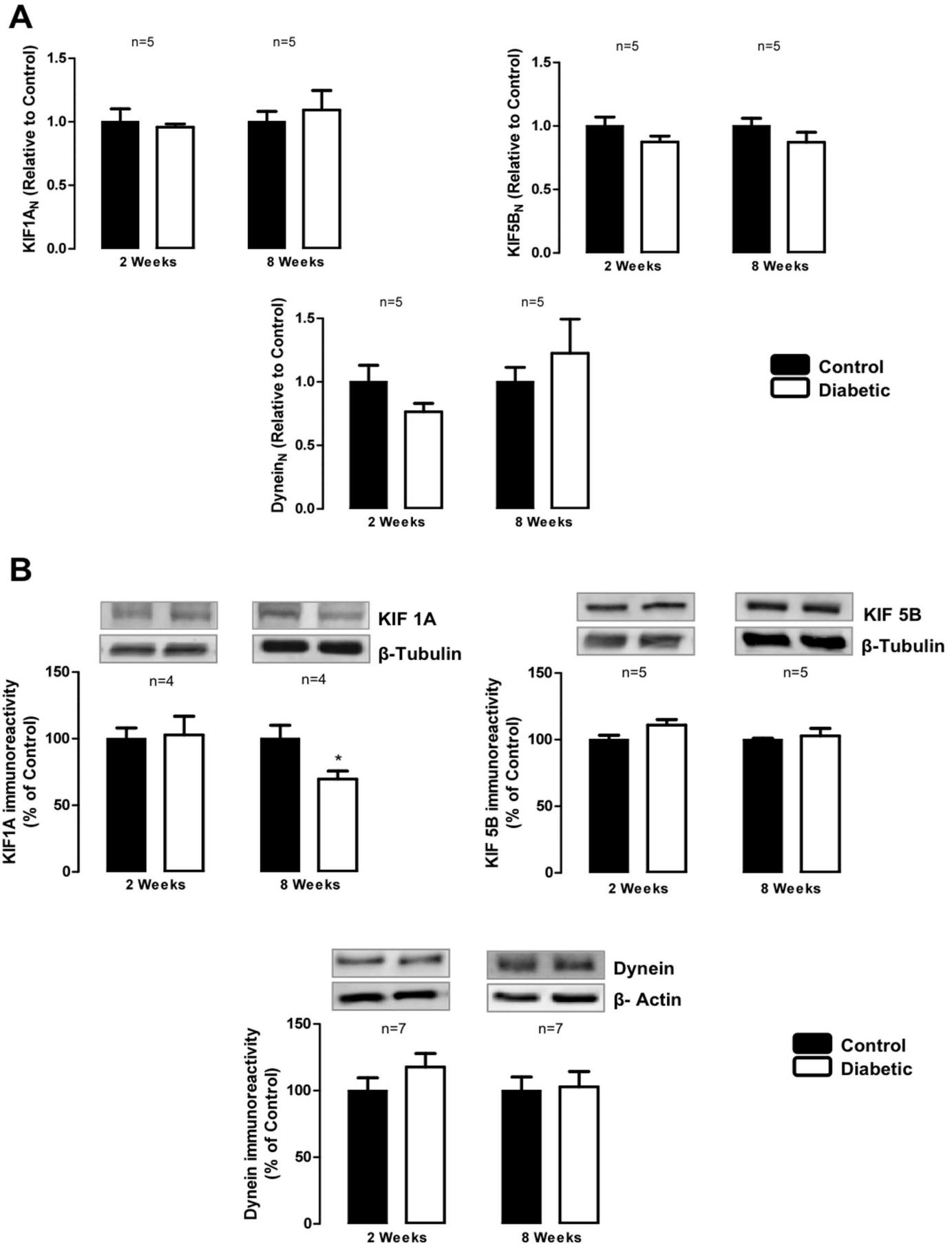
A
n=5
n=5
1.5
1.0
0.5
0.0
KIF1A$_N$ (Relative to Control)
2 Weeks
8 Weeks
n=5
n=5
KIF5B$_N$ (Relative to Control)
Dynein$_N$ (Relative to Control)
Control
Diabetic
B
KIF 1A
β-Tubulin
n=4
n=4
KIF1A immunoreactivity (% of Control)
150
100
50
0
*
KIF 5B
n=5
n=5
KIF 5B immunoreactivity (% of Control)
Dynein
β- Actin
n=7
n=7
Dynein immunoreactivity (% of Control)

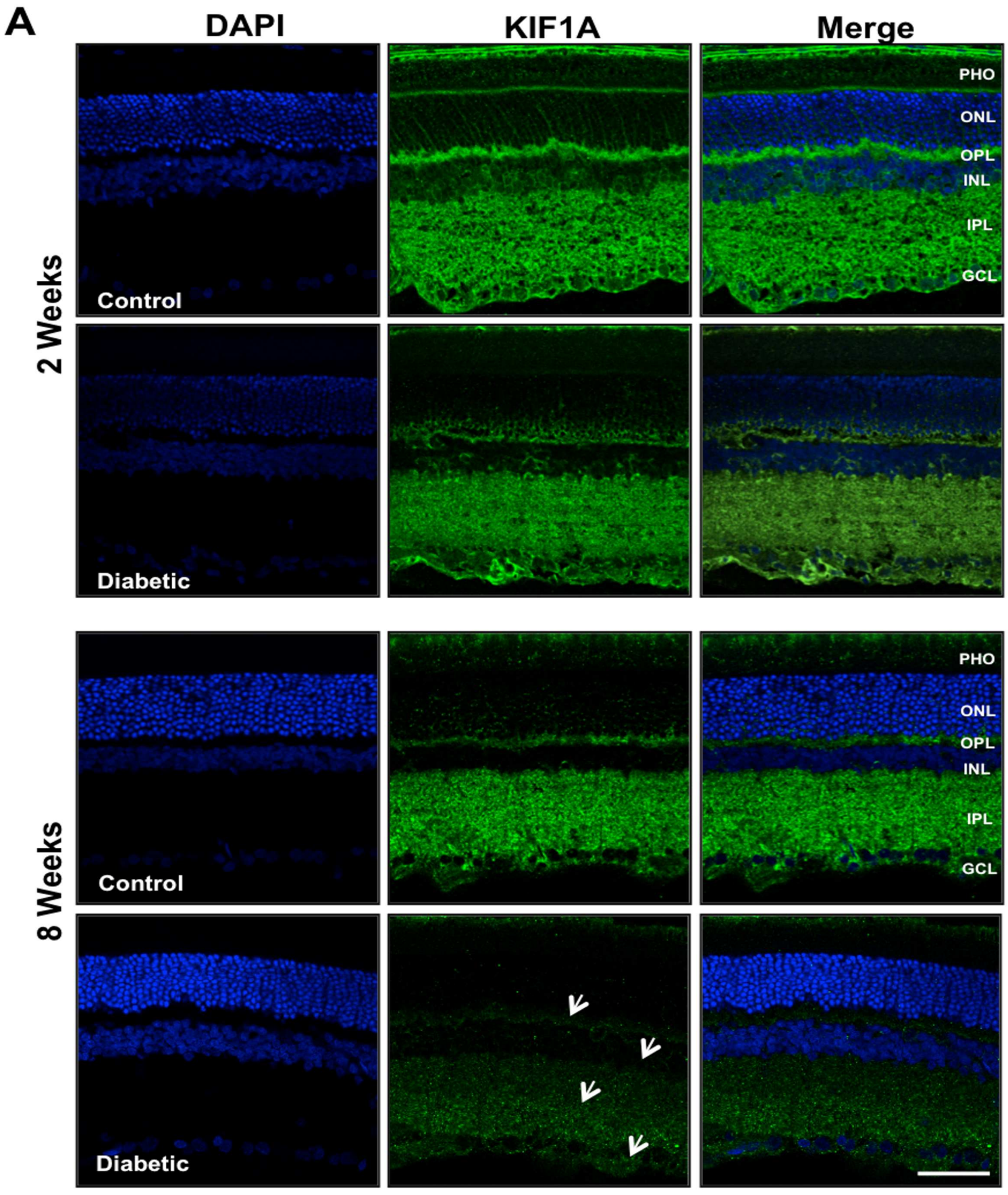
A
DAPI
KIF1A
Merge
PHO
ONL
OPL
INL
IPL
GCL
2 Weeks
Control
Diabetic
8 Weeks
Control
Diabetic

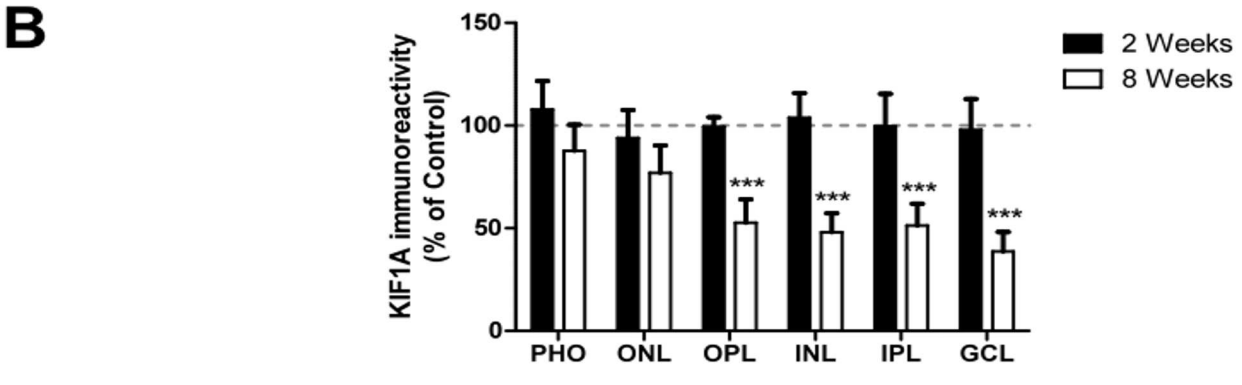
B
KIF1A immunoreactivity
(% of Control)
150
100
50
0
***
PHO
ONL
OPL
INL
IPL
GCL
2 Weeks
8 Weeks

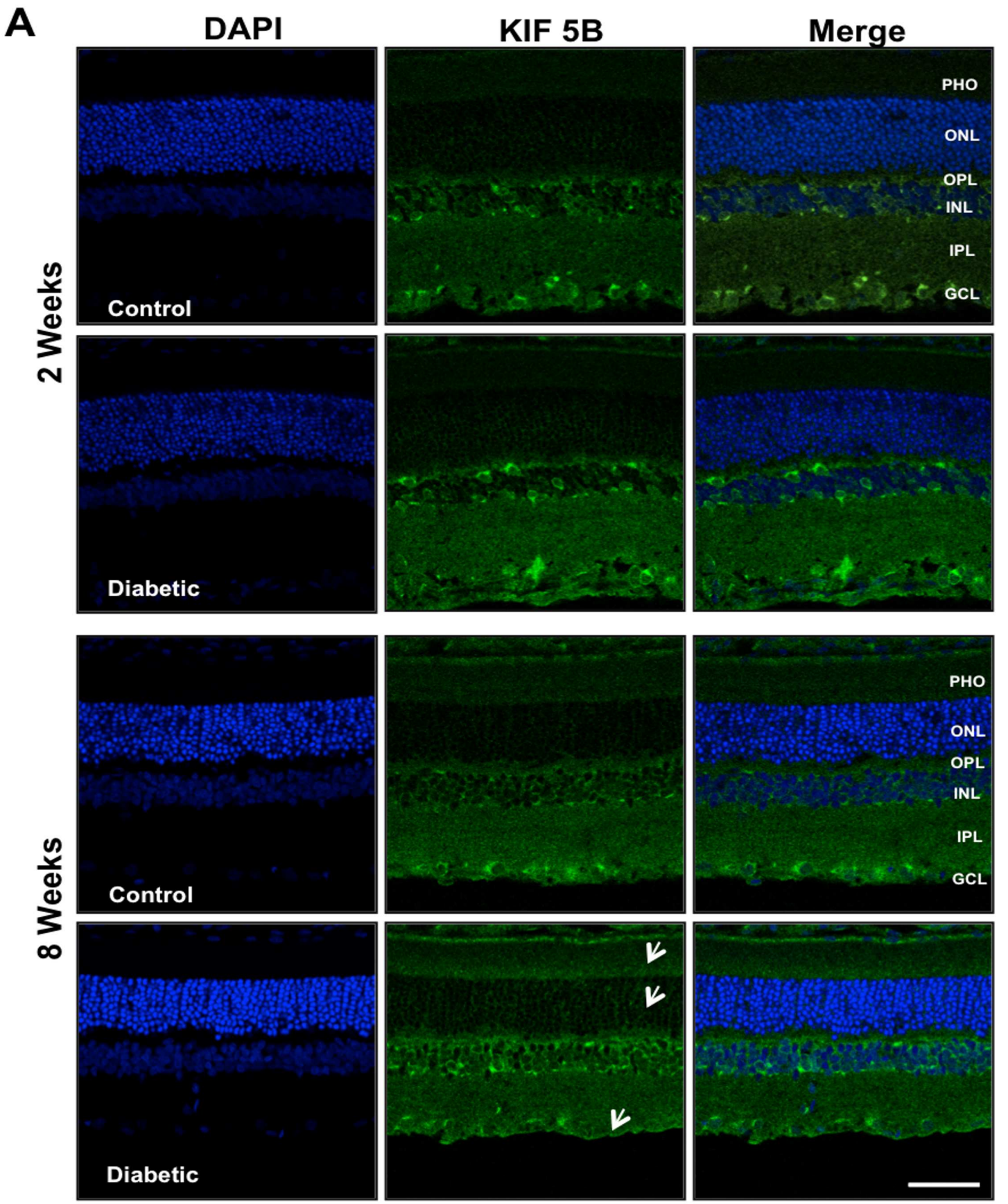
A
DAPI
KIF 5B
Merge
2 Weeks
8 Weeks
Control
Diabetic
Control
Diabetic
PHO
ONL
OPL
INL
IPL
GCL
PHO
ONL
OPL
INL
IPL
GCL

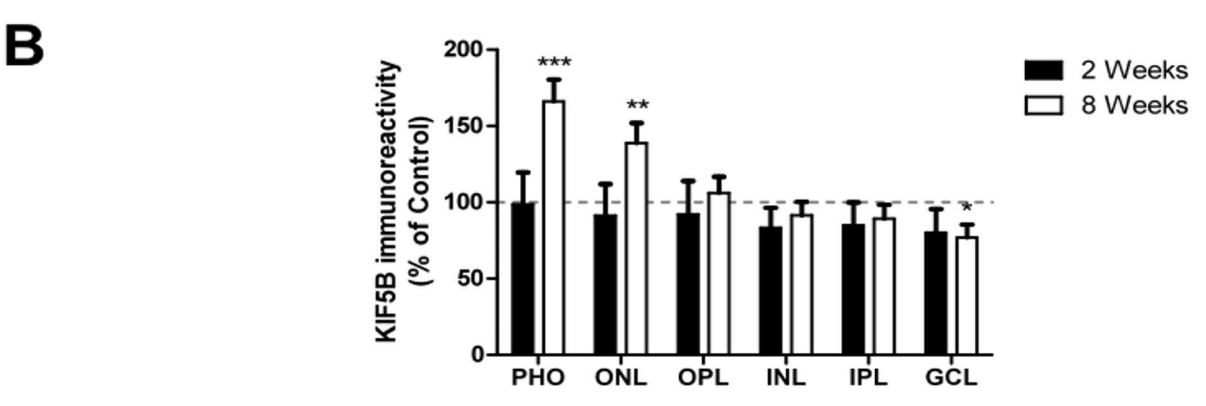
B
KIF5B immunoreactivity
(% of Control)
200
150
100
50
0
***
**
*
2 Weeks
8 Weeks
PHO
ONL
OPL
INL
IPL
GCL

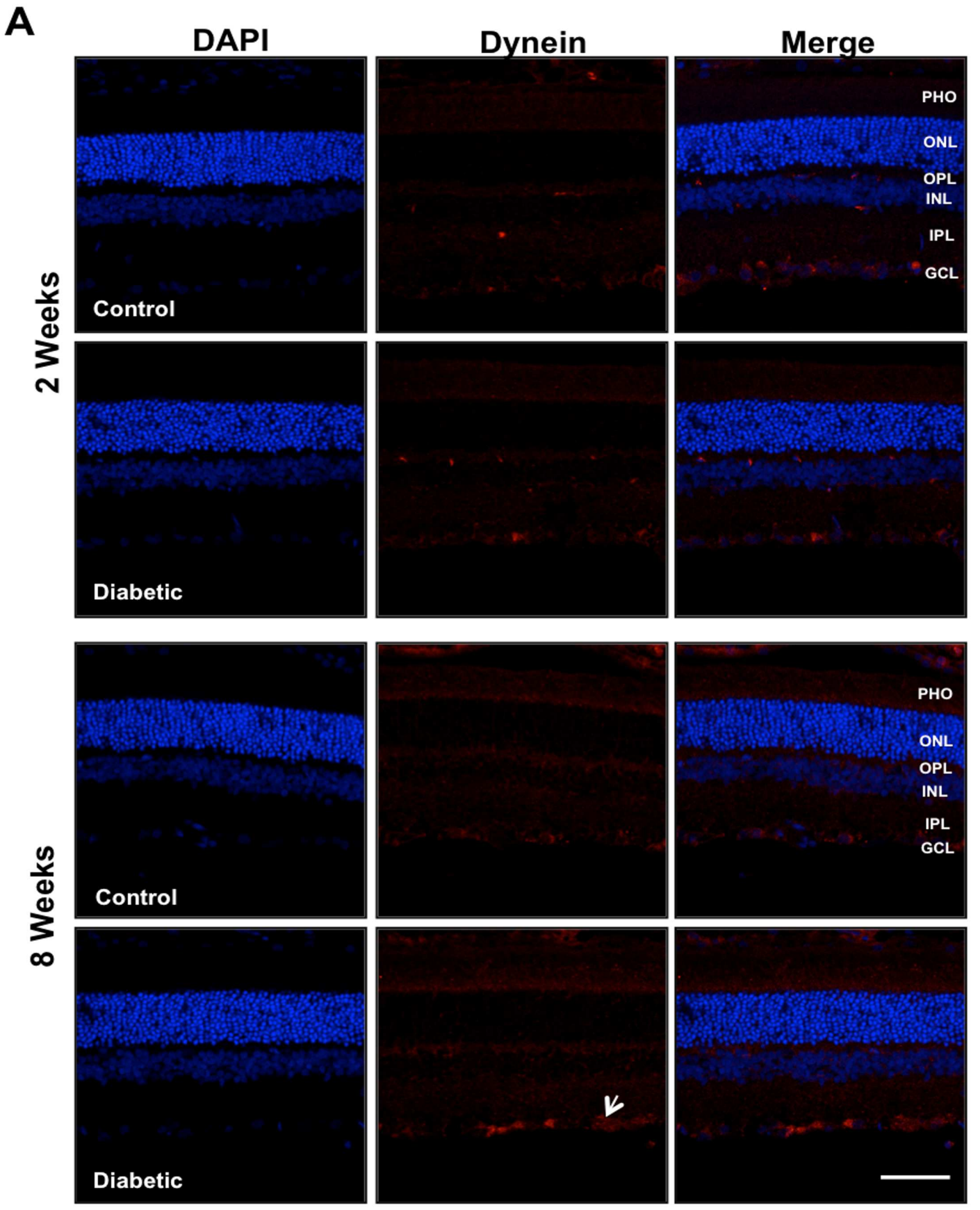
A
DAPI
Dynein
Merge
2 Weeks
Control
Diabetic
8 Weeks
Control
Diabetic
PHO
ONL
OPL
INL
IPL
GCL
B
Dynein immunoreactivity (% of Control)
150
100
50
0
PHO
ONL
OPL
INL
IPL
GCL
*
2 Weeks
8 Weeks

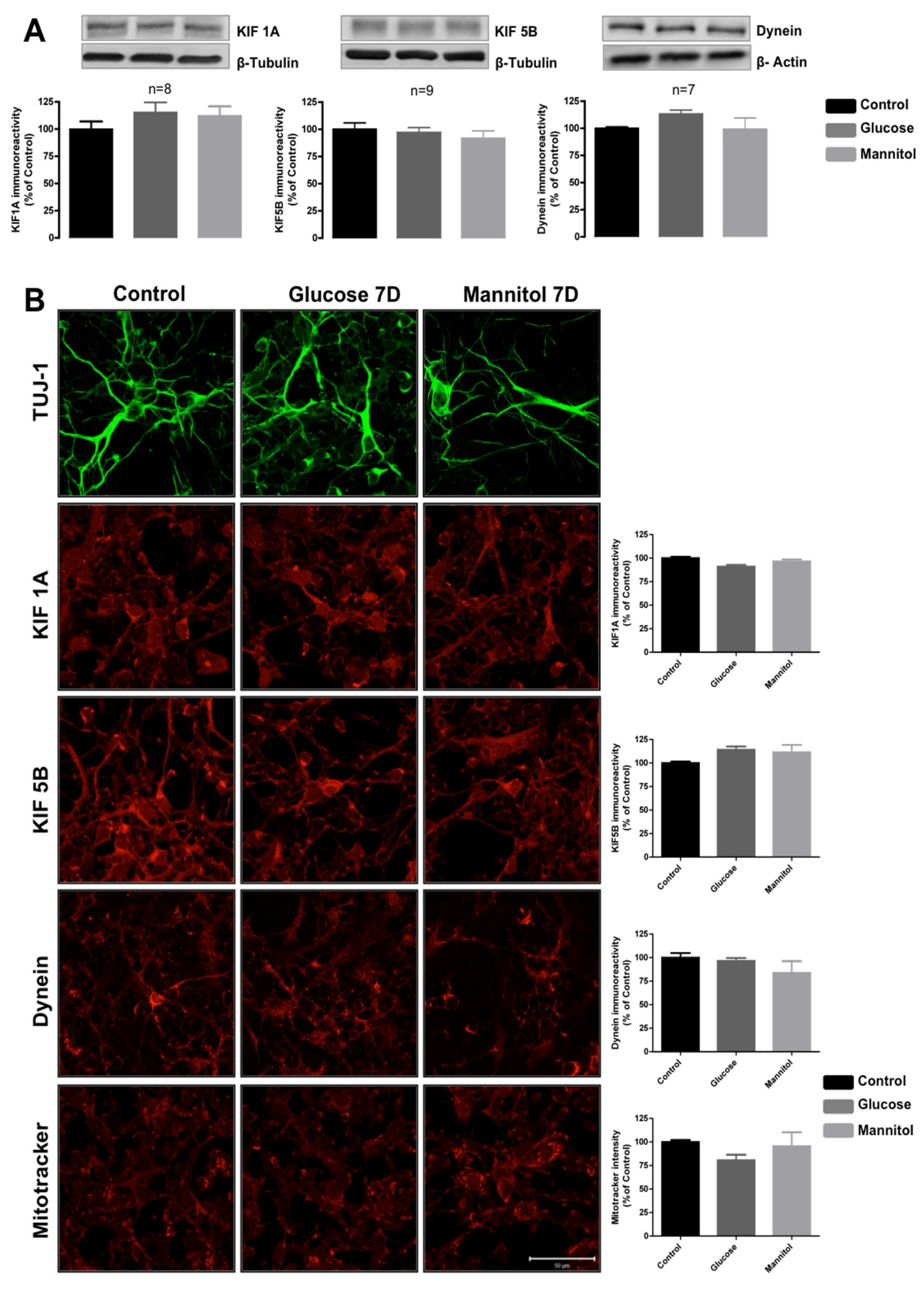
A
KIF 1A
β-Tubulin
KIF 5B
β-Tubulin
Dynein
β- Actin
n=8
n=9
n=7
KIF1A immunoreactivity (%of Control)
KIF5B immunoreactivity (%of Control)
Dynein immunoreactivity (% of Control)
125
100
75
50
25
0
Control
Glucose
Mannitol
B
Control
Glucose 7D
Mannitol 7D
TUJ-1
KIF 1A
KIF 5B
Dynein
Mitotracker
KIF1A immunoreactivity (% of Control)
KIF5B immunoreactivity (% of Control)
Dynein immunoreactivity (% of Control)
Mitotracker intensity (%of Control)
Control
Glucose
Mannitol
50 µm

Highlights:

- Kinesin and dynein motor proteins are altered in the retinas of diabetic rats.
- High glucose per se did not lead to changes in motor proteins in retinal neurons.
- Other factors, like inflammation, may contribute for the alterations in motor proteins.

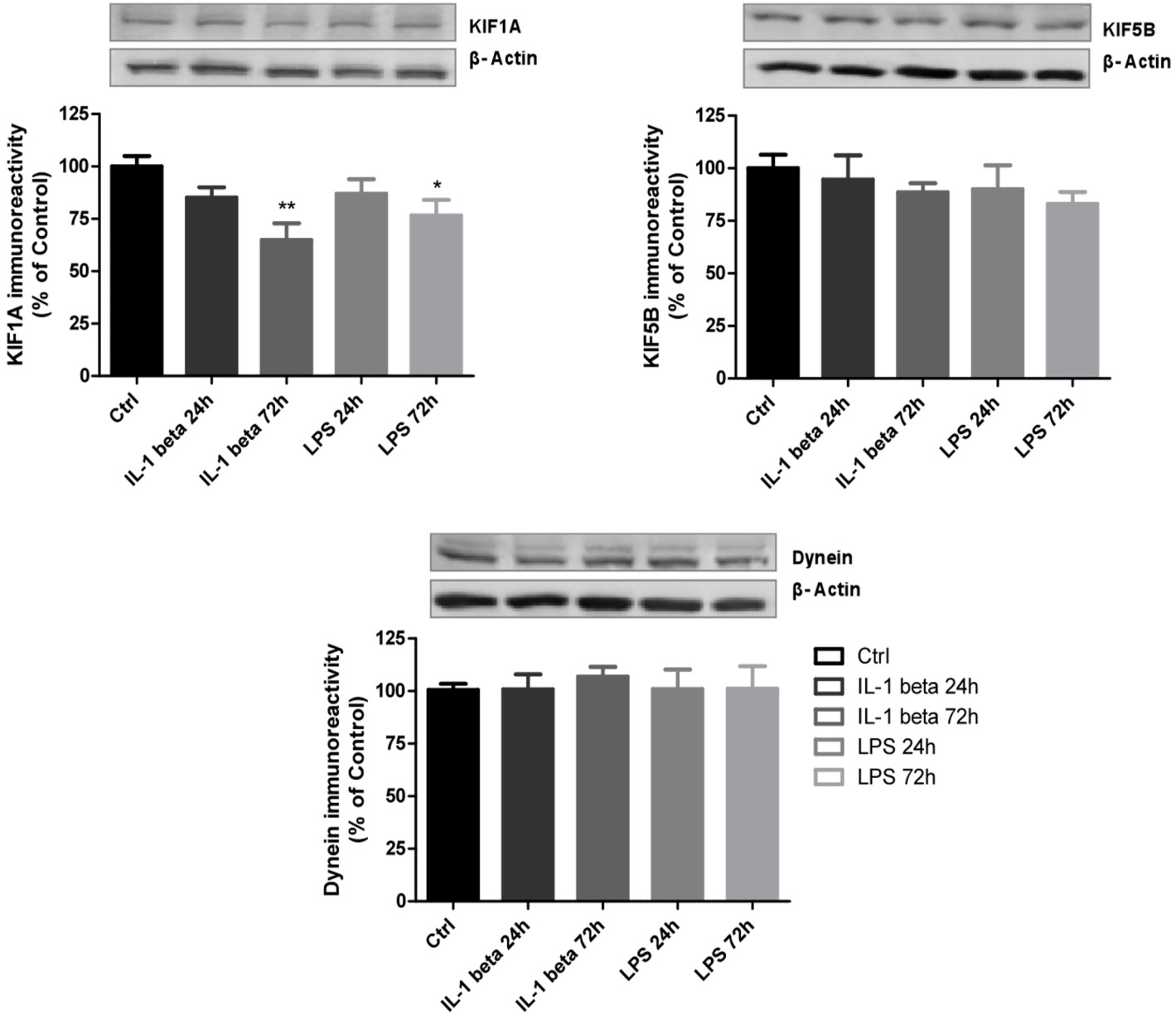
KIF1A
β-Actin
KIF1A immunoreactivity (% of Control)
125
100
75
50
25
0
**
*
Ctrl
IL-1 beta 24h
IL-1 beta 72h
LPS 24h
LPS 72h
KIF5B
β-Actin
KIF5B immunoreactivity (% of Control)
125
100
75
50
25
0
Ctrl
IL-1 beta 24h
IL-1 beta 72h
LPS 24h
LPS 72h
Dynein
β-Actin
Dynein immunoreactivity (% of Control)
125
100
75
50
25
0
Ctrl
IL-1 beta 24h
IL-1 beta 72h
LPS 24h
LPS 72h
Ctrl
IL-1 beta 24h
IL-1 beta 72h
LPS 24h
LPS 72h

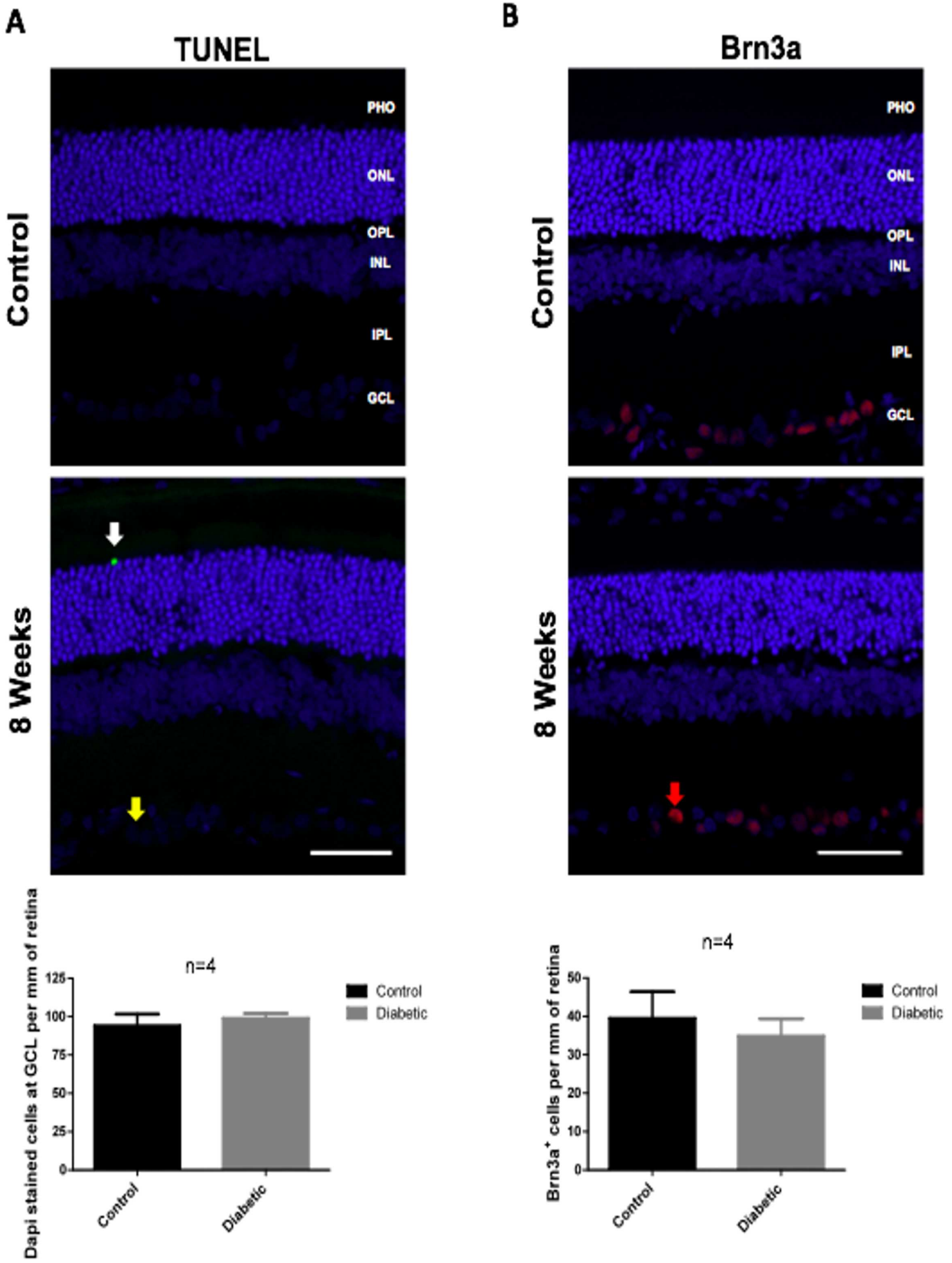
A
TUNEL
B
Brn3a
Control
8 Weeks
PHO
ONL
OPL
INL
IPL
GCL
n=4
Dapi stained cells at GCL per mm of retina
Brn3a+ cells per mm of retina
Control
Diabetic

C

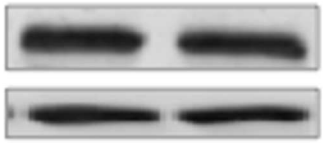
β- III Tubulin
β- Actin

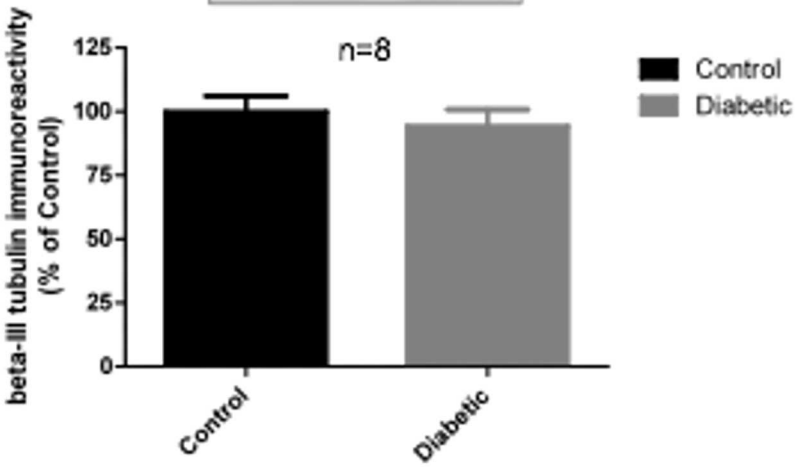
n=8
beta-III tubulin immunoreactivity (% of Control)
125
100
75
50
25
0
Control
Diabetic
Control
Diabetic

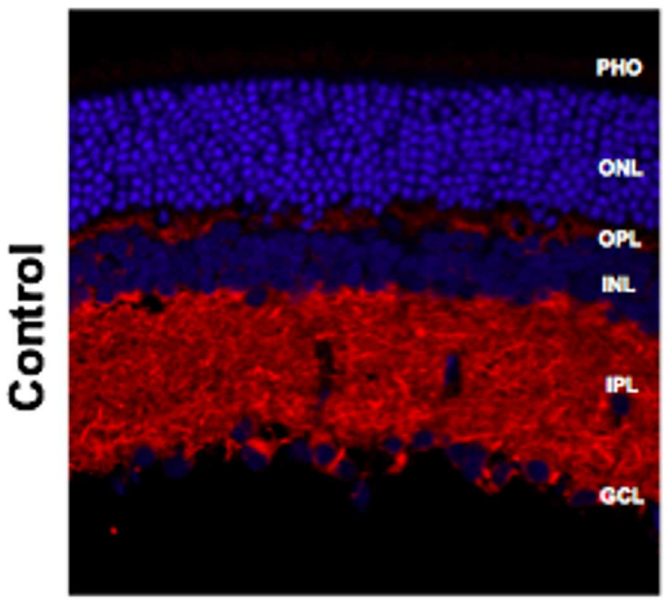
Control
PHO
ONL
OPL
INL
IPL
GCL

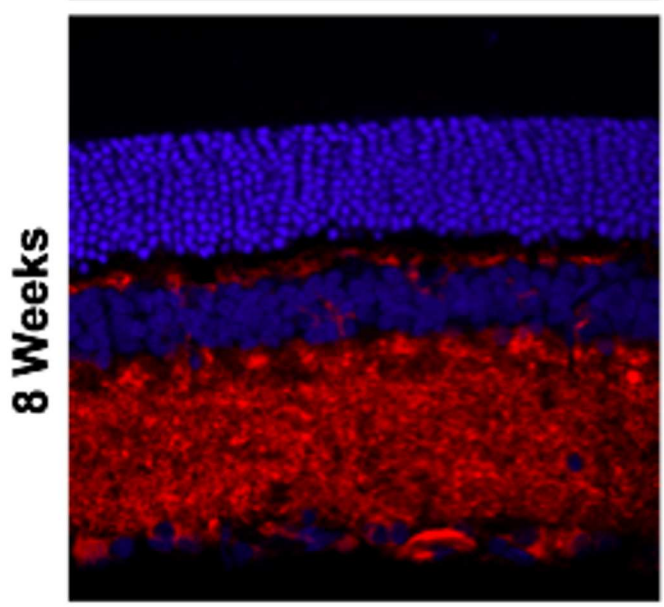
8 Weeks

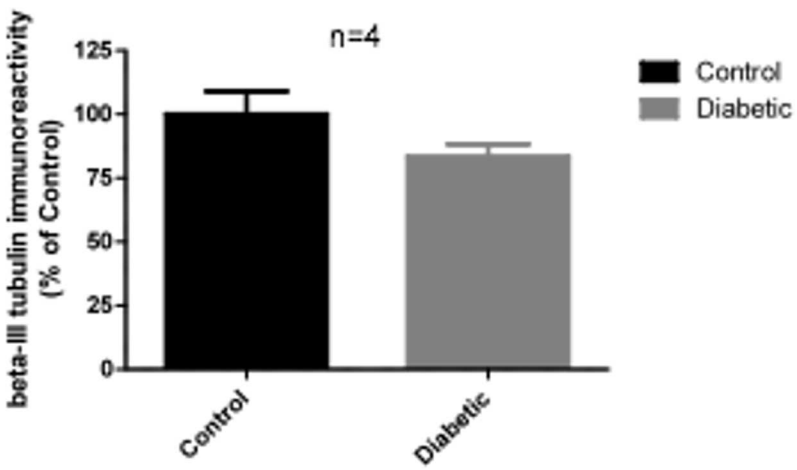
n=4
beta-III tubulin immunoreactivity (% of Control)
125
100
75
50
25
0
Control
Diabetic
Control
Diabetic

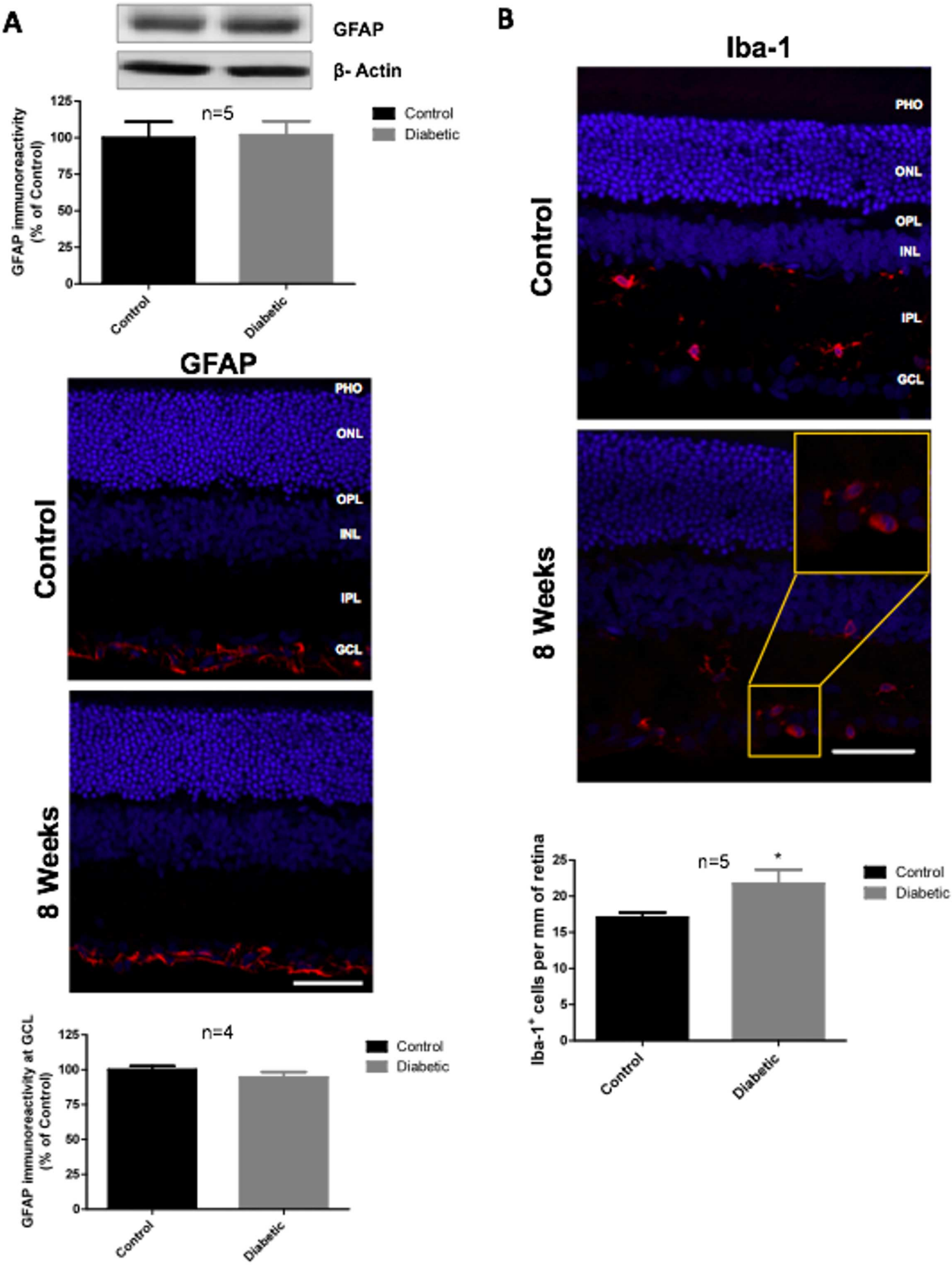
A
GFAP
β- Actin
n=5
Control
Diabetic
GFAP immunoreactivity (% of Control)
125
100
75
50
25
0
Control
Diabetic
GFAP
Control
8 Weeks
PHO
ONL
OPL
INL
IPL
GCL
n=4
Control
Diabetic
GFAP immunoreactivity at GCL (% of Control)
125
100
75
50
25
0
Control
Diabetic
B
Iba-1
Control
8 Weeks
PHO
ONL
OPL
INL
IPL
GCL
n=5
*
Control
Diabetic
Iba-1+ cells per mm of retina
25
20
15
10
5
0
Control
Diabetic